Mehran University Research Journal of Engineering and Technology

https://doi.org/10.22581/muet1982.2401.2917

2024, 43(1) 34-44

Comparative heat transfer analysis of Al_2O_3 and Cu nanoparticles based in H_2O nanofluids flow inside a C-shaped partially heated rectangular cavity

Muhammad Awais [a], Feroz Ahmed Soomro [b,*], Shreen El-Sapa [c], Rahim Bux Khokhar [d], Areej A. Almoneef [c]

[a] *Department of Mechanical Engineering, Quaid-e-Awam University of Engineering, Science and Technology, Larkana 77150, Sindh Pakistan*

[b] *Department of Mathematics, Xiamen University Malaysia, Sepang 43900, Selangor Malaysia*

[c] *Department of Mathematical Sciences, College of Science, Princess Nourah Bint Abdulrahman University, P. O. Box 84428, Riyadh 11671 Saudi Arabia*

[d] *Department of Basic Science and Related Studies, Mehran University of Engineering and Technology, Jamshoro 76062, Sindh Pakistan*

[*] Corresponding author: Feroz Ahmed Soomro, Email: ef.ey.soomro@gmail.com

Received: 12 July 2023, Accepted: 20 December 2023, Published: 01 January 2024

K E Y W O R D S

Heat Transfer Rate

Hybrid Nanofluid

Fluid-Structure Interaction

Partial Differential Equations

Finite Element Method

A B S T R A C T

The aim of the current study is to investigate the heat transfer performance of Al_2O_3 and Cu nanoparticles suspended based in H_2O nanofluids inside a partially heated C-shaped enclosure. The governing equations for heat and flow transfer are solved using the Finite Element Method. Heat transmission is affected by the type and form of nanoparticles. To study the improved heat transfer performance, four different shapes of nanoparticles-spherical, cylindrical, column, and lamina-have been used. The investigation showed that among the considered shapes of nanoparticles, the lamina shape of nanoparticles performed best. Considering lamina nanoparticles, in comparison to the simple nanofluids $Al_2O_3 - H_2O$ and $Cu - H_2O$ the hybrid nanofluid $Al_2O_3 - Cu - H_2O$ provides the enhanced heat transfer rate. The heat transfer is governed by convection at a higher Rayleigh number. On the other hand, the heat transfer rate is decreasing by increasing the impact of the magnetic field. For the increased heat transfer rate, the best choice is lamina nanoparticles and hybrid nanofluid $Al_2O_3 - Cu - H_2O$.

1. Introduction

The importance of heat transfer fluids to the industry and the variety of applications in physics and engineering have led to an increased focus on their thermal properties. Numerous academic studies have shown that the low surface to volume ratio for heat transfer, which results from the poor thermal conductivity of the majority of convectional fluids used for heat transfer, such as oil, ethylene glycol, water, and many others, limits the increase of heat transmission [1-3]. When it comes to the regulation and augmentation of heat inside closed geometries, it is crucial to keep in mind that heat may be added to or eliminated from a system. However, fluid is the best source to control a system's heating or cooling capability. There are several researches in the literature that use Choi's theory to increase the rate of heat transfer

[4-7]. Recently, a new category of nanofluids known as "hybrid nanofluids" was created, where several types of nanoparticles might be integrated into the base fluid. A thorough overview of hybrid nanofluids was provided by Kshirsagar et al. [8]. In practical applications, a cavity's size and form are frequently asymmetrical. Therefore, research into complicated enclosures and various aspect ratios is greatly encouraged in the field of fluid mechanics. Numerous studies on heat transmission and fluid movement are been out using various geometries, for instance Ahmed et al. [9] considered a lid-driven square cavity with hybrid nanofluids being transported convectively. Usman et al. [10] studied forced convection utilizing hybrid nanofluids inside a square cavity. A study on TiO_2 nanoparticles were carried out by Sreedevi et al. [11] to examine the effects of heat radiation and magnetic fields inside a square cavity. In a rectangular enclosure with heated wavy rods at either end, the natural convection of nanofluids was studied. Ullah et al. [12] analysis looked at the system's heat transmission and fluid flow parameters. Research on the transfer of heat and fluid flow inside cavities with an inner body have received significant attention recently because to their practical engineering applications, in addition to research employing nanofluids and diverse forms of cavities. Using hybrid nanofluids and various magnetic field strengths, Belhaj et al. [13] assessed the thermal performance of natural convection in a square container with an elliptical-shaped barrier. In a lid-driven cavity, trapezoidal chambers and triangular-shaped barriers were used in a study by Khan et al. [14]. The study focused on the application of hybrid nanofluids, in the trapezoidal chamber with a rotating body inside. Job et al. [15] did computational experiment on magneto hydrodynamic of unstable convective flow. Studies on other complicated shape cavities has also been reported. Jiang et al. [16], studied the heat transmission and entropy production of magnetohydrodynamic (MHD) hybrid nanofluids were investigated in a cubic chamber with wavy walls and rotating blocks. Usman et al. [17] reported the effects of various obstacles and radiation over the convection heat transfer phenomenon. Hamid et al. [18] carried out mathematical study over the non-Newtonian Prandtl fluid over a horizontal surface with slip effects to examine the natural convection heat transfer. Readers are suggested the articles [19-25] for further reading on the behaviour of heat transfer.

In the study of fluid dynamics and heat transmission, the Rayleigh number is a crucial variable, its capabilities include Designing heat transmission systems, predicting the commencement of convection, and researching fluid mechanics phenomena, for this reason numerous studies has been carried out, a few are citied below. Alumina and copper nanoparticles suspended in water were the subject of a numerical analysis by Parvin et al. [26] inside a chamber with a wavy-shaped cylinder. The results show that increasing the concentration of the hybrid nanofluid and Rayleigh number significantly increases the rate of thermal transmission; however, increasing the Hartmann number has the opposite effect. Nag et al. [27] numerically studied triangular enclosure which is heated at the corner, with different inclinations using Magnetohydrodynamic nanofluids. Using nanofluids with various frequencies, Yadav et al. [28] examine the impact of sinusoidal heating inside a square-shaped cavity. He also looked at a grooved enclosure that had a corner that was partially heated to look at low Reynolds number mixed convection of nanofluids [29]. In their research, Sen et al. [30] studied the behaviour of nanofluids with magnetohydrodynamic effects in a trapezoidal shaped enclosure subjected to irregular heating. The study considered the influence of the Rayleigh number, Hartmann number, and solid-volume percentage of alumina nanofluid. Study on ZnO, Fe_3O_4 and Al_2O_3 have been reported by Alam et al. [31] in which natural convection inside semi-circular cavity were considered. Rashid et al. [32] examined different shapes of nanofluids sphere, lamina and column in a square shaped enclosure with circular shape fin inside. The graphical outcomes show that Lamina shape nanoparticles perform better. Amine et al. [33] explored MHD effects of hybrid nanofluids inside in triangular cavity with quarter porous medium at one end, the obtained results show Rayleigh numbers increasing influence on heat transfer as well as the magnetic parameter's regulating function. Increases in the permeability and porosity of porous medium had a significant impact on how well heat was transported inside the enclosure. Hussain et al. [34] explored staggered cavity to see the MHD and Casson fluids impacts. Mohammad et al. [35] carried work on trapezoidal lid-driven cavity with different angle of inclinations using Hybrid nanofluids. Natural convection of hybrid nanofluids using lattice Boltzmann method was studied by Khan et al. [36]. Abdelaziz et al. [37] carried research on mixed convection of nanofluids, iconic nanofluids and hybrid nanofluids in a tube. Chabani et al. [38] considered a trapezoidal shape enclosure using hybrid nanoparticles the results of the

study revealed that in order to maximize heat transmission, Rayleigh number, solid-volume percentage, and Darcy should be raised, while Hartmann number must be decreased. In another study [39], he examined the impact of altering the Rayleigh number, volume fraction, speed of the revolving cylinder, and Hartmann number on a triangular cavity with zigzag and elliptic obstacles.

The comparative analysis of heat transfer between simple nanofluids and hybrid nanofluids plays a crucial role in determining the optimal working fluid. Hence, this article focuses on conducting a comparative heat transfer analysis of $Al_2O_3 - H_2O, Cu - H_2O, Al_2O_3 - Cu - H_2O$ nanofluids flowing inside a c-shape enclosure which is partially heated. An electromagnetic field and a portion of heating are applied to the cavity's left vertical wall. The Finite Element Method is used to solve the governing equations, which are a collection of nonlinear partial differential equations. The paper is organized into several sections. Section 1 provides an introduction to the background and previous studies related to the problem. The mathematical framework is outlined in Section 2. The applied numerical procedure is explained in Section 3. A detailed discussion on the obtained results is presented in Section 4. Finally, a comprehensive conclusion is provided in Section 5. The references cited in the manuscript are listed at the end in the references section.

2. Mathematical Formulation

This article focuses on performing a numerical study of a viscous fluid flowing steadily and incompressible in two dimensions inside a partially heated C-shaped cavity. The cavity is filled with three different types of nanofluids: namely $Al_2O_3 - H_2O$, $Cu - H_2O$ and and $Al_2O_3 - Cu - H_2O$. The left side of the cavity is kept at higher temperature while right side is at slightly lower temperature and all other sides are considered adiabatic. Fig.1 depicts the geometry of the described cavity. A transverse magnetic field is applied to the cavity, normal to its left heated boundary. Additionally, the consequences of viscous dissipation are also disregarded. The induced magnetic field is neglected due to low Reynolds number. Moreover, radiation and dissipation effects are also neglected. The following are the governing equations for the aforementioned criteria [40].

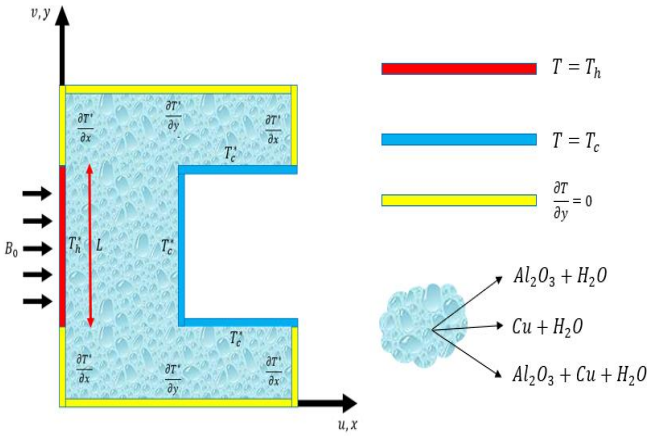

Fig. 1 illustrates a visual depiction of the physical problem

$$\frac{\partial u}{\partial x} + \frac{\partial v}{\partial y} = 0, \tag{1}$$

$$u\frac{\partial u}{\partial x} + v\frac{\partial u}{\partial y} = -\left(\frac{1}{\rho_{nf}}\right)\frac{\partial p}{\partial x} + \left(\frac{\mu_{nf}}{\rho_{nf}}\right)\left(\frac{\partial^2 u}{\partial x^2} + \frac{\partial^2 u}{\partial y^2}\right), \tag{2}$$

$$u\frac{\partial v}{\partial x} + v\frac{\partial v}{\partial y} = -\left(\frac{1}{\rho_{nf}}\right)\frac{\partial p}{\partial y} + \left(\frac{\mu_{nf}}{\rho_{nf}}\right)\left(\frac{\partial^2 v}{\partial x^2} + \frac{\partial^2 v}{\partial y^2}\right) + \frac{g(\rho\beta)_{nf}}{\rho_{nf}}(T^* - T_c^*) - \left(\frac{\sigma_{nf}}{\rho_{nf}}\right)B_0^2\, v, \tag{3}$$

$$u\frac{\partial T^*}{\partial x} + v\frac{\partial T^*}{\partial y} = \frac{k_{nf}}{(\rho C_p)_{nf}}\left(\frac{\partial^2 T^*}{\partial x^2} + \frac{\partial^2 T^*}{\partial y^2}\right). \tag{4}$$

where u and v are the respective velocity components along the x and $y - axis$, p is the pressure, g is the gravitational force, T^* is the temperature ($T_h^* > T_c^*$), and B_0 is the strength of magnetic field. Moreover, density ρ_{nf}, dynamic viscosity μ_{nf}, thermal expansion coefficient β_f, electric conductivity σ_{nf}, thermal conductivity k_{nf}, and specific heat capacity C_p are the thermophysical properties of nanofluid. These properties are computed using nano relations described in Table 1 and Table 2. $(\#)_1$, $(\#)_2$, and $(\#)_f$ shows the property of nanoparticles Al_2O_3, Cu, and base fluid H_2O, respectively and is described in Table 3. Thermal conductivity model involves the nanoparticles shape factor m, which is provided in Table 4. Moreover, the governing Eqs. 1-4 are coupled with the boundary conditions described in Table 5. Introducing the following nondimensional variables:

$$U = \frac{uL}{\alpha_f}, V = \frac{vL}{\alpha_f}, X = \frac{x}{L}, Y = \frac{y}{L},$$
$$P = \frac{pL^2}{\rho_f \alpha_f^2}, \; T = \frac{T^* - T_c^*}{T_h^* - T_c^*}, \alpha_f = \frac{k_f}{(\rho C_p)_f}, \nu_f = \frac{\mu_f}{\rho_f}, \tag{5}$$
$$Ra = \frac{\beta_f (T_h^* - T_c^*) L^3}{\nu_f \alpha_f}, Pr = \frac{\nu_f}{\alpha_f}, Ha = B_0 L\sqrt{\frac{\alpha_f}{\mu_f}}.$$

where L is the characteristic length of the heated boundary, α_f is the thermal diffusivity, ν_f is the kinematic viscosity, Ra is the Rayleigh number, Pr is the Prandtl number, and Ha is the Hartmann number. Utilizing the variables defined in Eq. 5, the Eqs. 1-4 takes the following nondimensional form.

$$\frac{\partial U}{\partial X}+\frac{\partial V}{\partial Y}=0, \tag{6}$$

$$U\frac{\partial U}{\partial X}+V\frac{\partial U}{\partial Y}=-\left(\frac{\rho_f}{\rho_{nf}}\right)\frac{\partial P}{\partial X}+\left(\frac{\nu_{nf}}{\nu_f}\right)Pr\left(\frac{\partial^2 U}{\partial X^2}+\frac{\partial^2 U}{\partial Y^2}\right), \tag{7}$$

$$U\frac{\partial V}{\partial X}+V\frac{\partial V}{\partial Y}=-\left(\frac{\rho_f}{\rho_{nf}}\right)\frac{\partial P}{\partial Y}+\left(\frac{\nu_{nf}}{\nu_f}\right)Pr\left(\frac{\partial^2 V}{\partial X^2}+\frac{\partial^2 V}{\partial Y^2}\right)+\frac{(\rho\beta)_{nf}}{\beta_f\rho_{nf}}\,Ra\,\mathrm{Pr}\,T-\left(\frac{\rho_f}{\rho_{nf}}\right)\left(\frac{\sigma_{nf}}{\sigma_f}\right)Ha^2\,Pr\,V, \tag{8}$$

$$U\frac{\partial T}{\partial X}+V\frac{\partial T}{\partial Y}=\frac{\alpha_{nf}}{\alpha_f}\left(\frac{\partial^2 T}{\partial X^2}+\frac{\partial^2 T}{\partial Y^2}\right). \tag{9}$$

The corresponding non-dimensional boundary conditions are given in Table 6. The local and average heat transfer rates are given by the following Nusselt number expressions:

$$Nu_{Loc}=-\frac{k_{nf}}{k_f}\frac{dT}{dX}, \tag{10}$$

$$Nu_{Avg}=\frac{1}{L}\int_L Nu_{Loc}\,dY \tag{11}$$

Table 1

Nano relations for nanofluid [40]

Property	Nano Relation
Dynamic Viscosity	$\mu_{nf}=\frac{\mu_f}{(1-\phi)^{2.5}}$
Density	$\rho_{nf}=(1-\phi_1)\rho_f+\phi_1\rho_1$
Coefficient of Thermal Expansion	$(\rho\beta)_{nf}=(1-\phi_1)(\rho\beta)_f+\phi_1(\rho\beta)_1$
Specific Heat Capacity	$(\rho C_p)_{nf}=(1-\phi_1)\left(\rho C_p\right)_f+\phi_1\ (\rho C_p)_1$
Thermal Conductivity	$\frac{k_{nf.}}{k_f}=\frac{k_1+(m-1)k_f-(m-1)\phi_1(K_f-k_1)}{k_1+(m-1)k_f+\phi_1(K_f-k_1)}$
Electrical Conductivity	$\frac{\sigma_{nf}}{\sigma_f}=1+\frac{3\left(\frac{\sigma_1}{\sigma_f}-1\right)\phi_1}{\left(\frac{\sigma_1}{\sigma_f}+2\right)-\left(\frac{\sigma_1}{\sigma_f}-1\right)\phi_1}$

Table 2

Nano relations for hybrid nanofluid [41]

Property	Nano Relation
Dynamic Viscosity	$\mu_{hnf}=\frac{\mu_f}{(1-\phi_1)^{2.5}(1-\phi_2)^{2.5}}$
Density	$\rho_{hnf}=(01-\phi_2)\left[(01-\phi_1)\rho_f+\phi_1\rho_1\right]+\phi_2\rho_2$
Coefficient of Thermal Expansion	$\rho_{hnf}=(01-\phi_2)\left[(01-\phi_1)\rho_f+\phi_1\rho_1\right]+\phi_2\rho_2$
Specific Heat Capacity	$\rho C_p)_{hnf}=(01-\phi_2)\left[(01-\phi_1)(\rho C_p)_f+\phi_1(\rho C_p)_1\right]+\phi_2(\rho C_p)_2$
Thermal Conductivity	$\frac{k_{hnf}}{k_{bf}}=\frac{k_2+(m-1)k_{bf}-(m-1)\phi_2(K_{bf}-k_2}{k_2+(m-1)k_{bf}+\phi_2(K_{bf}-k_2)}$ Where $\frac{k_{bf}}{k_f}=\frac{k_1+(m-1)k_f-(m-1)\phi_1(K_f-k_1)}{k_1+(m-1)k_f+\phi_1(K_f-k_1)}$
Electrical Conductivity	$\frac{\sigma_{hnf}}{\sigma_{bf}}=\frac{\sigma_2+2\sigma_{bf}-2\phi_2(\sigma_{bf}-\sigma_2)}{\sigma_2+2\sigma_{bf}+\phi_2(\sigma_{bf}-\sigma_2)}$ Where $\frac{\sigma_{bf}}{\sigma_f}=\frac{\sigma_1+2\sigma_f-2\phi_1(\sigma_f-\sigma_1)}{\sigma_1+2\sigma_f+\phi_1(\sigma_f-\sigma_1)}$

Table 3

Thermophysical properties of base fluid H_2O and nanoparticles Al_2O_3 and Cu. [42]

Property	H_2O	Al_2O_3	Cu
$\rho\ (kgm^{-3})$	997.1	3940	8933
$C_p\ (Jkg^{-1}K^{-1})$	4179	765	358
$k\ (Wm^{-1}K^{-1})$	0.613	40	400
$\beta(K^{-1})$	21×10^{-5}	0.85×10^{-5}	1.67×10^{-5}
$\sigma\ (\Omega^{-1}m^{-1})$	0.05	1×10^{-10}	5.96×10^{-7}
$\mu\ (kgm^{-1}s^{-1})$	8.9×10^{-4}	---	---
Pr	6.2	---	---

Table 4

Factor values of various shapes of nanoparticles

Shapes	Spherical	Cylindrical	Column	Lamina
Factor (m)	3	4.8	6.37	16.16

Table 5

Dimensional boundary conditions

Boundary	Velocity Condition	Temperature Condition
$x = 0, 0 \le y \le 0.25L$ and $0.75L \le y \le L$ $x = L, 0 \le y \le 0.25L$ and $0.75L \le y \le L$ $0 \le x \le L, y = 0.0$ $0 \le x \le L, y = L$	$u = v = 0$	$\frac{\partial T^*}{\partial x} = 0$
$x = 0.5L, 0.25L \le y \le 0.75L$	$u = v = 0$	$T^* = T_c^*$
$0.5L \le x \le L, y = 0.25L$ $0.5L \le x \le L, y = 0.75L$	$u = v = 0$	$T^* = T_h^*$

Table 6

Non-dimensional boundary conditions

Boundary	Velocity Condition	Temperature Condition
$X = 0, 0 \le Y \le 0.25$ and $0.75 \le Y \le 1$ $X = 1, 0 \le Y \le 0.25$ and $0.75 \le Y \le 1$ $0 \le X \le 1, Y = 0$ $0 \le X \le 1, Y = 1$	$U = V = 0$	$\frac{\partial T}{\partial X} = 0$
$X = 0.5, 0.25 \le Y \le 0.75$ $0.5 \le X \le 1, Y = 0.25$ $0.5 \le X \le 1, Y = 0.75$	$U = V = 0$	$T = 0$
$X = 0, 0.25 \le Y \le 0.75$	$U = V = 0$	$T = 1$

3. Solution Procedure and Validation

The well-known numerical method known as the Finite Element Method (FEM) utilizing the Galerkin approach is used to solve the governing Eqs. 6–9 and the accompanying boundary conditions. The procedures for applying FEM in simulation are as follows:

i. The space domain is discretised into triangular elemental mesh

ii. Derivation of elemental equations

iii. Assembly of elemental equations

iv. Applying boundary conditions

v. Solution of assembled equations

The fundamentals and procedure about the approach is well described by Dechaumphai [43] and Taylor and Hood [44]. The pressure term P may be eliminated from the Eqs. 7, 8 by the following continuity constraint equation:

$$P = -\gamma\left(\frac{\partial U}{\partial X} + \frac{\partial V}{\partial Y}\right) \tag{12}$$

For large values of γ ($\gamma = 10^7$) equation for continuity is satisfied. The space domain is discretised into the finite number of triangular elements (see Fig. 2(a)). The impact of number of nodes on the average Nusselt number can be seen from Fig. 2(b). To validate the applicability of the obtained solutions, the code is tested on the experimental results published by Calcagni et al. [45] (Fig. 3). Strong agreement between the results shows the validity of the presented solutions.

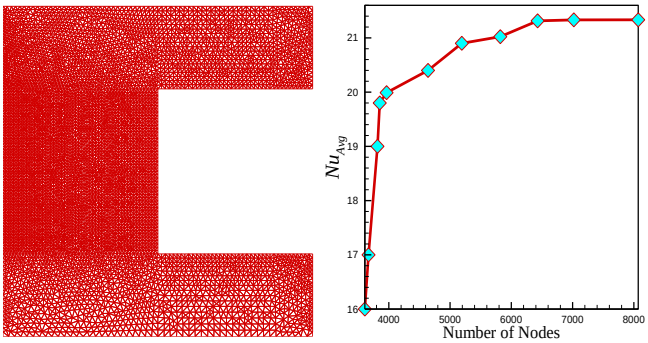

Fig. 2. (a) Triangular mesh, and (b) mesh sensitivity curve

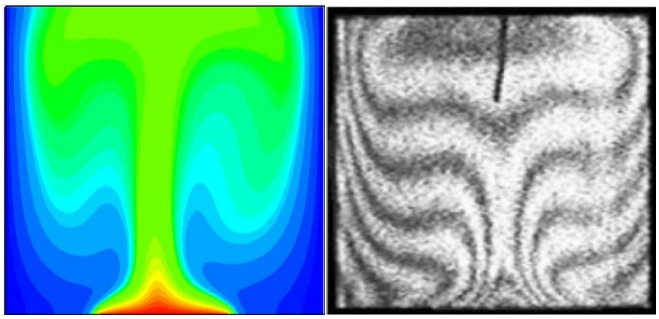

Fig. 3. Comparison of present work with existing experimental work when $L_T = 0.4,\ \phi = 0\ ,\ and\ Ra = 1.85 \times 10^5$

4. Results and Discussion

The Finite Element Method is used to find the numerical solution. Mathematical framework of the considered problem gives rise to physical parameters, such as Rayleigh number and Hartmann number, which greatly affect the flow and heat transfer. The simulation

is performed for the ranges $10^4 \leq Ra \leq 10^6$ and $0 \leq Ha \leq 100$. The distribution of flow and temperature inside the cavity is determined from the results. To further analyse the behaviour of heat transmission at the heated length of the cavity, the local and average Nusselt numbers are determined. Isotherms and streamlines are used to demonstrate the flow and temperature distribution. While the line graphs are used for Nusselt number computation.

The simulation examines the local Nusselt numbers for a variety of nanoparticle shapes, including spherical, cylindrical, column, and lamina particles. The lamina-shaped nanoparticles outperform other shapes in heat transfer, according to the numerical analysis results, which are depicted in Fig. 4(a). The lamina shape has an average Nusselt number of 21.42, followed by column shapes with 12.86, cylinder shapes with 11.20, and spheres with 9.19. Moreover, average Nusselt number is shown in Fig. 4(b) which shows the values for three different types of nanofluids: $Al_2O_3 - H_2O$, $Cu - H_2O$ *and* $Al_2O_3 - Cu - H_2O$ hybrid nanofluid. It is important to emphasize that water is used as the base fluid in these tests. The graph makes it very evident that the $Al_2O_3 - Cu - H_2O$ hybrid nanofluid has the highest Nusselt number values, coming in at 18.43. On the other hand, it is revealed that the values of average Nusselt numbers for the other nanofluids, namely $Al_2O_3 - H_2O$ *and* $Cu - H_2O$ are 9.65 and 8.26, respectively.

These findings show the considerable impact of nanoparticle shape and type of nanofluid on heat transmission properties. Compared to the other forms examined in this work, laminate-shaped nanoparticles exhibit greater heat transmission performance. Additionally, the $Al_2O_3 - Cu - H_2O$ hybrid nanofluid has the greatest average Nusselt number, indicating improved heat transmission capability. Designing effective heat transfer systems requires a thorough understanding of the effects of various nanoparticle shapes and nanofluid compositions on heat transmission. The study's findings progress the development of improved systems that use particular nanoparticle sizes and formulations of nanofluids to increase heat transfer rates. In conclusion, these findings highlight the importance of choosing the right nanoparticle shape and nanofluid for enhancing heat transfer performance. Based on these findings, future research and optimizations can be made to investigate new nanoparticle forms and varied nanofluid compositions, ultimately improving the efficiency of heat transfer in a variety of applications.

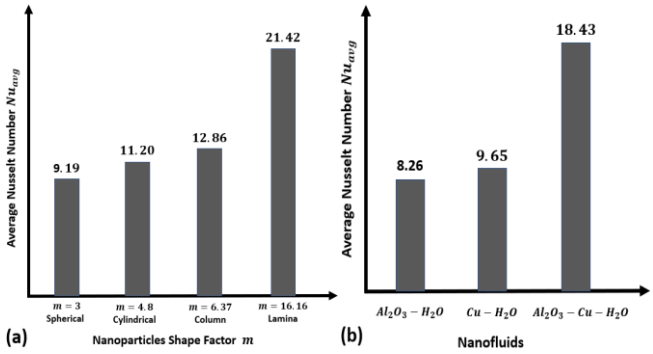

Fig. 4. Average Nusselt number under the impact of (a) nanoparticles of different shapes, and (b) different nanofluids

4.1 Impact of increasing the values Rayleigh number considering the of $Al_2O_3 - Cu - H_2O$ hybrid nanofluid

Fig. 5(a) and (b) use streamlines and isotherm plots, respectively, to show how the Rayleigh number affects the flow and temperature distribution. Conduction is the primary mode of heat transfer at low Rayleigh numbers, and the flow field is weak. The effect of increasing the Rayleigh number intensifies the flow field, indicating a shift towards convective heat transfer. When the value of Rayleigh number is kept low then the isotherm plots shows that the temperature distribution is uniform, primarily influenced by conduction. However, when the values of Rayleigh numbers are set to a higher number, the isotherms become twisted and exhibit significant fluctuations, indicating the effect of convective heat transport and non-uniform temperature distribution. Furthermore, Fig. 5(a)-(c) demonstrates that the flow field inside the C-shaped cavity, revealing a distinct difference in flow field intensity between the top and lower regions. This variation can be attributed to the placement of higher temperature source on the left vertical wall of the cavity which ultimately causes the heated fluid to rise and concentrate the flow in the upper section, while the cooler right wall attracts the hot fluid, resulting in a flow concentration towards the right. Fig. 5(d)-(f) depict the effect of the increasing the values of Rayleigh number on temperature distribution within the cavity, showing that when the values of Rayleigh number is set to a higher value, the distribution of temperature becomes more influenced by convective effects, causing the isotherms to deviate from their initial parallel orientation.

Additionally, Fig. 6(a)-(b) presents the line graphs illustrating the relationship between the Rayleigh number, Nusselt number (characterizing convective heat transfer), and temperature. The graphs demonstrate that

higher Rayleigh numbers facilitate more effective convective heat transmission within the enclosure. Moreover, the rate of heat transmission is non-uniform along the partly heated wall and the mean horizontal route, with variations between the upper and lower sections of the enclosure. In conclusion, the images shed light on the fluid's behaviour within the C-shaped cavity by emphasizing the impact of the heat location and Rayleigh number on the flow pattern, temperature distribution, and heat transfer properties. According to the findings, buoyancy effects have a major impact on the flow field and temperature distribution within the cavity, changing from a dominantly conductive mode at low Rayleigh numbers to a dominant convective mode at higher Rayleigh numbers.

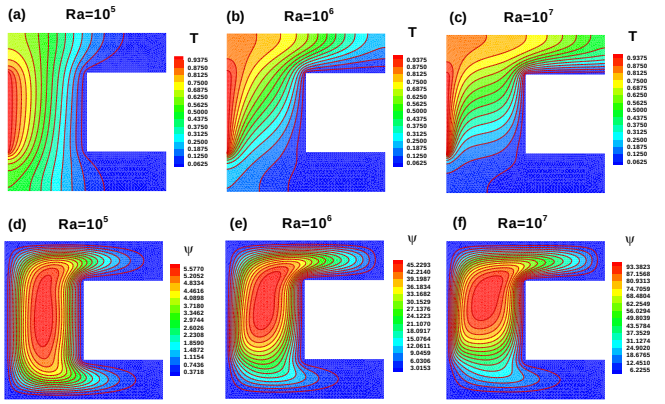

Fig. 5. Effect of Increasing Rayleigh number under the influence of $Al_2O_3 - Cu - H_2O$ Hybrid Nanofluid

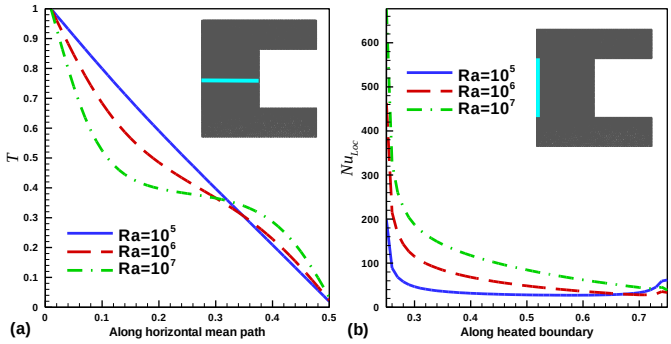

Fig. 6. Effect of Increasing Rayleigh number in mean path and heated length under the influence of $Al_2O_3 - Cu - H_2O$ hybrid nanofluid

4.2 Impact of increasing the values Hartmann number

The effect of magnetic field strength, as measured by the Hartmann number (Ha), on the flow field and temperature distribution inside a cavity is examined in the section that follows. These impacts are examined using streamlines, isotherm plots, and Nusselt number profiles. A stronger flow field results from raising the Hartmann number, as seen in Fig. 7(a)–(c). When $Ha = 0$, streamlines are parallel to the borders and the flow core is centered within the cavity. The flow field, however, extends and covers a larger area of the cavity as the Hartmann number rises, as seen in Fig. 7(c) for $Ha = 100$. Convection is the main method of heat transport, as evidenced by the temperature distribution in Fig. 7(d)–(f). As seen in Fig. 7(d), convective heat transfer from the heated area on the left vertical wall causes the upper half of the cavity to grow hotter. Heat transfer rates decline with increasing Hartmann numbers, and conductive heat transfer takes over with a Hartmann number of 100.

The Nusselt number profiles are shown in Fig. 8, which shows how the heat transfer rate fluctuates in relation to the Hartmann number. As the Hartmann number rises, the heat transmission reduces, as shown in Fig. 8(a). As a result, conduction is the main mechanism by which the fluid surrounding the heated portion warms up. Furthermore, the passage briefly mentions the behaviour of flow velocities at different points within the cavity. The horizontal velocity near the heated wall decreases with increasing Hartmann number, primarily due to the magnetic field's constraining effect on the flow. Conversely, at locations farther from the heated area, an inverse behaviour is observed, indicating an increase in horizontal velocity, likely caused by flow redistribution induced by the magnetic field. The vertical velocity profiles exhibit asymmetrical behaviour, suggesting that the vertical velocities on both sides of the cavity follow a similar pattern, indicating the influence of comparable elements or mechanisms.

In conclusion, the impact of magnetic field strength, as measured by the Hartmann number, on the flow field and temperature distribution inside a cavity is covered in this section. The streamlines and isotherm plots show that the flow field weakens with increasing Hartmann number and switches from convective to conductive heat transfer. The Nusselt number profiles show that when the Hartmann number rises, the rate of heat transmission decreases. The chapter also addresses the asymmetric behaviour seen in vertical velocity profiles and fluctuations in horizontal velocity near the heated wall.

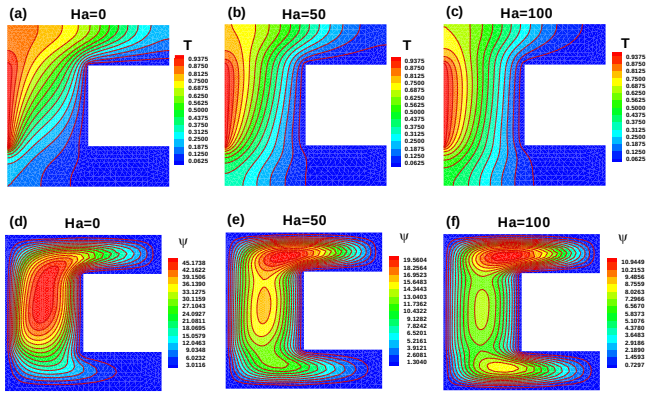

Fig. 7. Effect of increasing Hartmann number under the influence of $Al_2O_3 - Cu - H_2O$ nanofluid

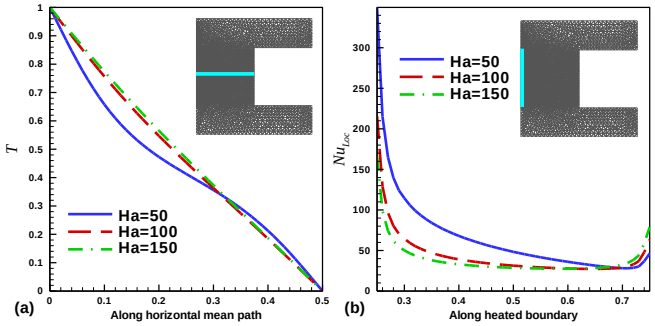

Fig. 8. Temperature and Nusselt Number along mean position and heated length

5. Conclusion

This study compared the heat transfer properties of Al_2O_3 *and* Cu nanoparticles suspended in water-based nanofluids. The flow was taken into consideration inside the magnetically exposed, C-shaped enclosure that had been partially heated. The Finite Element Method with Galerkin Approach is used to find the solution to the governing equations. To achieve improved heat transfer performance, a thorough investigation is carried out for a variety of new physical characteristics, including the Rayleigh number (Ra) and Hartmann number (Ha) for different forms of nanoparticles. The study concludes that in comparison to simple nanofluids $Al_2O_3 - H_2O$ and $Cu - H_2O$, the hybrid nanofluid $Al_2O_3 - Cu - H_2O$ provides the enhanced heat transfer behavior. Moreover, lamina shape of nanoparticles works best to obtain the maximum heat transfer rate. At lower values Rayleigh numbers, heat transfer primarily occurs through conduction, while at higher values of Rayleigh numbers, convection becomes the dominant heat transfer mechanism. Higher values of the Hartmann number equate to a stronger magnetic field, resulting in less fluid movement.

6. Declaration of Competing Interests

The authors declare that they have no known competing financial interests or personal relationships that could have appeared to influence the work reported in this paper.

7. Acknowledgment

Princess Nourah bint Abdulrahman University through researchers supporting Project number (PNURSP2023R154), Princess Nourah bint Abdulrahman University, Riyadh, Saudi Arabia.

8. References

[1] H. Younes, M. Mao, M. Murshed, and D. Lou, "Key parameters to enhance thermal conductivity and its applications," Applied Thermal Engineering, vol. 207, pp. 118202, 2022, doi.org/10.1016/j.applthermaleng.2022.118202.

[2] H. Lin, Q. Jian, X. Bai, D. Li, Z. Huang, W. Huang, S. Feng, and Z. Cheng, "Recent advances in thermal conductivity and thermal applications of graphene and its derivatives nanofluids," Applied Thermal Engineering, vol. 218, pp. 119176, 2023, doi.org/10.1016/j.applthermaleng.2022.119176.

[3] W.E. Ukueje, F.I. Abam, and A. Obi, "A perspective review on thermal conductivity of hybrid nanofluids and their application in automobile radiator cooling," Journal of Nanotechnology, vol. 2022, pp. 2187932, 2022,doi.org/10.1155/2022/2187932

[4] K. Thirumalaisamy and S.Ramachandran, "Comparative heat transfer analysis on $Fe_3O_4 - H_2O$ and $Fe_3O_4 - Cu - H_2O$ flow inside a tilted square porous cavity with shape effects." Physics of Fluids, vol. 35, pp. 022007, 2023, doi.org/10.1063/5.0136326

[5] K. Thirumalaisamy, S. Ramachandran, V.R. Prasad, O. A. Bég, H.H. Leung, F. Kamalov, and R.P. Selvam. "Comparative heat transfer analysis of electroconductive $Fe_3O_4 - MWCNT -$ water and $Fe_3O_4 - MWCNT - Kerosene$ hybrid nanofluids in a square porous cavity using the non-Fourier heat flux model." Physics of Fluids, vol. 34, no. 12, pp. 122016, 2022, doi.org/10.1063/5.0127463

[6] S. Alqaed, J. Mustafa, F.A. Almehmadi, and M. Sharifpur, "Numerical study of entropy generation in the convection heat transfer of nanofluid inside a tilted closed compartment

with five constant-temperature heat sources in the presence of a magnetic field," Engineering Analysis with Boundary Elements, vol. 150, pp. 329-341, 2023 doi.org/10.1016/j.enganabound.2023.02.019

[7] R. Sarlak, A.M. Abed, O.A. Akbari, A. Marzban, S. Baghaei, and M. Bayat. "Numerical investigation of natural convection heat transfer of water/SWCNT nanofluid flow in a triangular cavity with cold fluid injection." Progress in Nuclear Energy, vol. 155, pp. 104513, 2023, doi.org/10.1016/j.pnucene.2022.104513

[8] D.P. Kshirsagar and M.A. Venkatesh, "A review on hybrid nanofluids for engineering applications," Materials Today: Proceedings, vol. 44, pp. 744-755, 2021, doi.org/10.1016/j.matpr.2020.10.637

[9] S. Ahmed, H. Xu, Y. Zhou, and Q. Yu, "Modelling convective transport of hybrid nanofluid in a lid driven square cavity with consideration of Brownian diffusion and thermophoresis," International Communications in Heat and Mass Transfer, vol. 137, pp. 106226, 2022, doi.org/10.1016/j.icheatmasstransfer.2022.106226

[10] A.A. Memon, H. Anwaar, T. Muhammad, A.A. Alharbi, A.S. Alshomrani, and Y.R Aladwani, "A forced convection of water-aluminum oxide nanofluids in a square cavity containing a circular rotating disk of unit speed with high Reynolds number A Comsol Multiphysics study," Case Studies in Thermal Engineering, vol. 39, pp. 102370, 2022, doi.org/10.1016/j.csite.2022.102370

[11] P. Sreedevi and P.S. Reddy, "Effect of magnetic field and thermal radiation on natural convection in a square cavity filled with TiO_2 nanoparticles using Tiwari-Das nanofluid model," Alexandria Engineering Journal, vol. 61(2), pp. 1529-1541, 2022, doi.org/10.1016/j.aej.2021.06.055

[12] N. Ullah, S. Nadeem, and A.U. Khan, "Finite element simulations for natural convective flow of nanofluid in a rectangular cavity having corrugated heated rods," Journal of Thermal Analysis and Calorimetry, vol. 143, pp. 4169-4181, 2021, doi.org/10.1007/s10973-020-09378-4

[13] S. Belhaj and B.B. Beya, "Thermal performance analysis of hybrid nanofluid natural convection in a square cavity containing an elliptical obstacle under variable magnetic field," International Journal of Numerical Methods for Heat and Fluid Flow," vol. 32, no. 6, pp. 1825-1860, 2022, doi.org/10.1108/HFF-04-2021-0300

[14] Z.H. Khan, W.A. Khan, M. Qasim, S.O. Alharbi, M. Hamid, and M. Du, "Hybrid nanofluid flow around a triangular-shaped obstacle inside a split lid-driven trapezoidal cavity," The European Physical Journal Special Topics, vol. 231, no. 13, pp. 2749-2759, 2022, 10.1140/epjs/s11734-022-00607-5

[15] V.M. Job, S.R. Gunakala, and A.J. Chamkha, "Numerical investigation of unsteady MHD mixed convective flow of hybrid nanofluid in a corrugated trapezoidal cavity with internal rotating heat-generating solid cylinder," The European Physical Journal Special Topics, vol. 231, no.13, pp. 2661-2668, 2022, doi.org/10.1140/epjs/s11734-022-00604-8

[16] X. Jiang, M. Hatami, A. Abderrahmane, O. Younis, B.M. Makhdoum, and K. Guedri, "Mixed convection heat transfer and entropy generation of MHD hybrid nanofluid in a cubic porous cavity with wavy wall and rotating cylinders," Applied Thermal Engineering, vol. 226, pp. 120302, 2023, doi.org/10.1016/j.applthermaleng.2023.120302

[17] M. Usman, Z.H. Khan, and M.B. Liu, "MHD natural convection and thermal control inside a cavity with obstacles under the radiation effects," Physica A: Statistical Mechanics and Its Applications, vol. 535, 2019, doi.org/10.1016/j.physa.2019.122443

[18] M. Hamid, T. Zubair, M. Usman, Z.H. Khan, and W. Wang, "Natural convection effects on heat and mass transfer of slip flow of time-dependent Prandtl fluid," Journal of Computational Design and Engineering, vol. 6, no. 4, pp. 584-592, 2019, doi.org/10.1016/j.jcde.2019.03.004

[19] M. Hamid, M. Usman, Z.H. Khan, R.U. Haq, and W. Wang, "Numerical study of unsteady MHD flow of Williamson nanofluid in a permeable channel with heat source/sink and thermal radiation," The European Physical

Journal Plus, vol. 133, no, 12, pp. 527, 2018, doi.org/10.1140/epjp/i2018-12322-5

[20] M. Hamid, M. Usman, Z.H. Khan, R. Ahmad, and W. Wang, "Dual solutions and stability analysis of flow and heat transfer of Casson fluid over a stretching sheet," Physics Letters A, vol. 383, no. 20, pp. 2400-2408, 2019, doi.org/10.1016/j.physleta.2019.04.050

[21] M. Hamid, M. Usman, T. Zubair, R.U. Haq, and A. Shafee, "An efficient analysis for N-soliton, Lump and lump–kink solutions of time-fractional(2+1)-Kadomtsev–Petviashvili equation," Physica A: Statistical Mechanics and its Applications, vol. 528, pp.121320, 2019, doi.org/10.1016/j.physa.2019.121320

[22] S.O. Alharbi, U. Khan, A. Zaib, A. Ishak, Z. Raizah, S.M. Eldin, and I. Pop, "Heat transfer analysis of buoyancy opposing radiated flow of alumina nanoparticles scattered in water-based fluid past a vertical cylinder," Scientific Reports, vol. 13, no. 1, pp. 10725, 2023, doi.org/10.1038/s41598-023-37973-6

[23] U. Khan, A. Zaib, A. Ishak, E.S.M. Sherif, I.E Sarris, S.M. Eldin, and I. Pop, "Analysis of assisting and opposing flows of the Eyring Powell fluid on the wall jet nanoparticles with significant impacts of irregular heat source/sink," Case Studies in Thermal Engineering, vol. 49, pp. 103209, 2023, doi.org/10.1016/j.csite.2023.103209

[24] U. Khan, A. Zaib, J.K. Madhukesh, S. Elattar, S.M. Eldin, A. Ishak, A. Raizah, and I. Waini, "Features of radiative mixed convective heat transfer on the slip flow of nanofluid past a stretching bended sheet with activation energy and binary reaction," Energies, vol. 15, no. 20, pp. 7613, 2022, doi.org/10.3390/en15207613

[25] U. Khan, A. Zaib, A. Ishak, SM. Eldin, A.M. Alotaibi, Z. Raizah, I. Waini, S. Elattar, and A.M. Abed, "Features of hybridized AA7072 and AA7075 alloys nanomaterials with melting heat transfer past a movable cylinder with Thompson and Troian slip effect," Arabian Journal of Chemistry, vol. 16, no. 2, pp. 104503, 2023, doi.org/10.1016/j.arabjc.2022.104503

[26] S. Parvin, N.C. Roy, and L.K. Saha, ''Magnetohydrodynamic natural convection of a hybrid nanofluid from a sinusoidal wavy cylinder placed in a curve-shaped cavity,'' AIP Advances, vol. 11, no. 8, pp. 085029, 2021, doi.org/10.1063/5.0061503

[27] S. Nag, N. Sen, H.T. Bamboowala, N.K. Manna, N. Biswas, and D.K. Mandal, "MHD nanofluid heat transport in a corner-heated triangular enclosure at different inclinations," Materials Today: Proceedings, vol. 63, pp. 141-148, 2022, doi.org/10.1016/j.matpr.2022.02.421

[28] C.K. Yadav, A. Halder, S. Mukherjee, N.K. Manna, N. Biswas, and D.K. Mandal, "Effect of sinusoidal heating and Hartmann number on nanofluid based heat flow evolution in a cavity," Materials Today: Proceedings, vol. 63, pp. 157-163, 2022, doi.org/10.1016/j.matpr.2022.02.434

[29] C.K. Yadav, K. Dey, N. K. Manna, and N. Biswas, "Low Reynolds number MHD mixed convection of nanofluid in a corner heated grooved cavity," Materials Today: Proceedings, vol. 63, pp. 170-175, 2022, doi.org/10.1016/j.matpr.2022.02.434

[30] N. Sen, S. Nag, H.T. Bamboowala, N.K. Manna, N. Biswas, D.K.Mandal, "Magnetohydrodynamic thermal behavior of nanofluid flow in a trapezoidal cavity subjected to non-uniform heating," Materials Today: Proceedings, vol. 63, pp. 320-327, 2022, doi.org/10.1016/j.matpr.2022.03.144

[31] M. S. Alam, M. M. Billah, S. M. C. Hossain, S. S. Keya, and M. M. Haque, "MHD influence on convective heat transfer in a semi-circular cavity using nonhomogeneous nanofluid model, International Journal of Thermofluids," vol. 16, 2022, doi.org/10.1016/j.ijft.2022.100197

[32] U. Rashid, D. Lu, and Q. Iqbal, "Nanoparticles impacts on natural convection nanofluid flow and heat transfer inside a square cavity with fixed a circular obstacle," Case Studies in Thermal Engineering, vol. 44, pp. 102829, 2023, doi.org/10.1016/j.csite.2023.102829

[33] B.M. Amine, F. Redouane, L. Mourad, W. Jamshed, M.R. Eid, and W.A. Kouz, "Magnetohydrodynamics natural convection of a triangular cavity involving Ag-MgO/water hybrid nanofluid and provided with rotating circular barrier and a quarter circular porous medium at its right-angled corner," Arabian Journal for Science and Engineering, vol. 46, no.

12, pp. 12573-12597, 2021, doi.org/10.1007/s13369-021-06015-6

[34] S.Hussain, S. Shoeibi, and T. Armaghani, "Impact of magnetic field and entropy generation of Casson fluid on double diffusive natural convection in staggered cavity," International Communications in Heat and Mass Transfer, vol. 127, pp. 105520, 2021, doi.org/10.1016/j.icheatmasstransfer.2021.105520

[35] A.A. Mohammed and M. Thaer "Mixed Convection Heat Transfer of $Al_2O_3 - H_2O$ Nanofluid in a Trapezoidal Lid-driven Cavity at Different Angles of Inclination," Texas Journal of Engineering and Technology, vol. 11, pp. 20-30, 2022

[36] N.H. Khan, M.K. Paswan, and M.A. Hassan, "Natural convection of hybrid nanofluid heat transport and entropy generation in cavity by using Lattice Boltzmann Method," Journal of the Indian Chemical Society, vol. 99, 2022, pp. 100344, doi.org/10.1016/j.jics.2022.100344

[37] A.H. Abdelaziz, W.M. El-Maghlany, A.A. El-Din, and M.A. Alnakeeb, "Mixed convection heat transfer utilizing Nanofluids, ionic Nanofluids, and hybrid nanofluids in a horizontal tube," Alexandria Engineering Journal, vol. 61, no. 12, pp. 9495-9508, 2022, doi.org/10.1016/j.aej.2022.03.001

[38] I. Chabani, F. Mebarek-Oudina, H. Vaidya, A.I. Ismail, "Numerical analysis of magnetic hybrid Nano-fluid natural convective flow in an adjusted porous trapezoidal enclosure," Journal of Magnetism and Magnetic Materials, vol. 564, pp. 170142, 2022, doi.org/10.1016/j.jmmm.2022.170142

[39] I. Chabani, F.M. Oudina, and A.A. Ismail, "MHD Flow of a Hybrid Nano-Fluid in a Triangular Enclosure with Zigzags and an Elliptic Obstacle," Micromachines, vol. 13 no. 24, pp. 224, 2022, doi.org/10.3390/mi13020224

[40] R.U. Haq, F.A. Soomro, H.F. Oztop, and T. Mekkaoui, "Thermal management of water-based carbon nanotubes enclosed in a partially heated triangular cavity with heated cylindrical obstacle," International Journal of Heat and Mass Transfer, vol. 131, pp. 724-736, 2019, doi.org/10.1016/j.ijheatmasstransfer.2018.11.090

[41] K. Thirumalaisamy and S. Ramachandran, "Comparative heat transfer analysis on $Fe_3O_4 - H_2O$ and $Fe_3O_4 - Cu - H_2O$ flow inside a tilted square cavity with shape factor," Physics of Fluids, vol. 35, pp. 022007, 2023, doi.org/10.1063/5.0136326

[42] F.A. Soomro, M. Usman, S. El-Sapa, M. Hamid, and R.U. Haq, "Numerical study of heat transfer performance of MHD $Al_2O_3 - Cu/$ water hybrid nanofluid flow over inclined surface," Archive of Applied Mechanics, vol. 92, pp. 2757-2765, 2022, doi.org/10.1007/s00419-022-02214-1

[43] P. Dechaumphai and W. Kanjanakijkasem. "A finite element method for viscous incompressible thermal flows," ScienceAsia vol. 25 pp. 165-172, 1999,

[44] C. Taylor and P. Hood, "A numerical solution of the Navier-Stokes equations using finite element technique," Computers and Fluids, vol.1, pp.73-89, 1973, doi.org/10.1016/0045-7930(73)90027-3

[45] B. Calcagni, F. Marsili, and M. Paroncini, "Natural convective heat transfer in square enclosures heated from below," Applied Thermal Engineering, vol. 25, pp. 2522-2531, 2005, doi.org/10.1016/j.applthermaleng.2004.11.032

